



## An Investigation of Microstructure and Mechanical Properties of Different Nano - Particles Doped Sn-Zn Lead-Free Solder Alloys

R. Afify Ismail

Physics department, Faculty of Science, Ain Shams University, Cairo, Egypt.

Received 24<sup>th</sup> Jun. 2019  
Accepted 22<sup>nd</sup> Dec. 2019

This study investigates the effect of two different nano-particle additions; namely copper oxide (CuO) and/or titanium oxide (TiO<sub>2</sub>) in modifying the properties of Sn-9wt. % Zn lead free solder alloy. The composite approach has been developed to enhance the microstructure and mechanical properties of lead free solder. The microstructure before and after alloy modification was investigated. The results indicated that 1wt.% of either CuO and /or TiO<sub>2</sub> lead to microstructure refinement due to the the nanosized reinforced particles which dispersed uniformly in the solder matrix. A significant improvement is achieved by 1 wt.% TiO<sub>2</sub> addition to Sn-9wt. % Zn. In the current work, the studies have extended to show the effect of different aging temperatures (75, 100, 125, 150 °C) on the solder alloy doped with 1wt.% TiO<sub>2</sub>. An anomalous effect was shown at the aging temperature of 100°C due to the dissolution of Zn-metal in the β-Sn rich phase. The stress exponent values for the solder alloy doped with TiO<sub>2</sub> were found to vary with aging temperatures between (4.7-14.9) respectively.

**Keywords:** Lead-free solders, TiO<sub>2</sub> and CuO nano-particles, Sn-Zn based alloy, microstructure, tensile creep properties

### Introduction

Due to the realization of the harmful influence of Pb on the human health, efforts had been conducted to search for suitable Pb-free solders as a replacement for the conventional Pb-Sn eutectic alloy [1-4]. Therefore many researchers were concerned with the development of new lead free solders by adding appropriate second phase particles to the solder matrix to form a composite. The reliability is mainly dependent on matching the coefficient of thermal expansion and having good mechanical properties [5]. Recently, nanocomposite solders have been developed for the electronic packaging materials industry to improve the microstructures and thermo mechanical fatigue resistance of solder joints to be used in service at high temperature [6-14]. Mc Cormack and Jin have pointed to the Sn-9Zn alloy as a non toxic binary lead free solder that has excellent mechanical properties [15]. The

influence of reinforcing TiO<sub>2</sub> and Al<sub>2</sub>O<sub>3</sub> nanoparticles on the microstructure of eutectic Sn-Ag-Cu solders has been studied by L.C. Taso, S.Y.Chang, and Taso et. al [16,17]. They found that the addition of TiO<sub>2</sub> and/or Al<sub>2</sub>O<sub>3</sub> nanoparticle is helpful in enhancing the overall strength of the eutectic solder. The creep properties of Sn-xZn solders (x=9, 20, 25 wt.%) were studied by Shrestha et al.[18] and it was found that the solders exhibited stress exponents of about 5.0 and the mean value of activation energy for creep (66.3 kJ/mol.) They also identified creep mechanism at low temperature to be viscous glide of dislocations. Mavoori et al. [19] studied the creep characteristics of Sn-Zn eutectic solder at (323 K and 353 K) and indicated that the activation energies were in agreement with the activation energy for self-diffusion in pure tin (100 kJ/mol), suggesting creep mechanisms controlled by

dislocation climb. Hamada et al. [20] studied the creep behavior of Sn and Sn-xZn ( $x=0.1$  wt.% and 0.4 wt.%) in the temperature range between 298 and 398 K and under constant strain rates. They concluded that the addition of Zn improves the creep resistance of Sn, and found the stress exponent value to be equal to 7, suggesting the controlling mechanism is a dislocation pipe diffusion. El-Daly et al. [21] investigated the effect of Ni and Sb additions on the microstructure, thermal and mechanical properties of Sn-9 wt.% Zn. They pointed out that the values of the stress exponent and activation energies were consistent with those quoted for dislocation climb. Creep tests of Sn-8.8 wt.% Zn and Sn- 8.8 wt.% Zn-1.5 wt.% Ag solders were performed under different stresses and at the deformation temperatures ranging from 291 to 343 K by Saad et. al. [22] They found that the minimum creep rate of the solders increased with increasing applied stress and/or deformation temperature. As et.al and Tai et.al [23,24] showed significant improvement in the creep resistance on adding 1.5 wt.% Ag nano sized particle to the binary Sn- 8.8 wt.% Zn solder alloy. The composite approach has been developed to enhance the microstructure and mechanical properties, where the Ag nano sized particles act as pinning centers for the dislocation movements. Xing et al. [25] studied the mechanical and micro structural development of eutectic Sn-9Zn composite solders reinforced with nano-sized  $Al_2O_3$  particles. They concluded that the overall strength of the composite solders reinforced with  $Al_2O_3$  nanoparticles increased with increased content of  $Al_2O_3$ . Yassin et.al. [26] studied the effect of the addition of  $TiO_2$  with different proportional from 0.25 to 1.0 wt. % and two aging times (15 and 120 min) at one temperature 393K to Sn-6.5wt.%Zn, and obtained  $TiO_2$  with two phases, one of them is anatase for the low proportional  $TiO_2$  and rutile for the addition of 1.0wt.%  $TiO_2$ .

In the present work an attempt is made to show the effect of nano oxides (CuO and/or  $TiO_2$ ) addition on the microstructure and mechanical properties of the Sn-9wt.%Zn matrix material.

### Experimental Procedures

The Sn- 9wt.%Zn solder was prepared from molten Sn and Zn (99.9) purity in a furnace at 723K for two hours under argon atmosphere to

prevent vaporization of Zn. To form a cylindrical ingot of 10 mm diameter the molten solder was cast into a stainless steel mold. The Sn-9wt.%Zn-1wt.%CuO and Sn-9wt.%Zn-1wt.% $TiO_2$  composite were prepared by mechanically dispersing 1.0 wt.% of either CuO and/or  $TiO_2$  nano particles into Sn-9wt.% Zn solder. The composite solders were re-melted in a vacuum furnace under argon flow at 723 K for two hours, followed by casting into stainless steel molds to get a homogenous composition. The rod-like samples of 10 mm diameter were swaged into wires with gauge diameter of 0.8 mm for creep tests, and cold drawn into sheets for morphological studies.

The three alloy samples Sn- 9wt.%Zn, Sn-9wt.%Zn-1wt.%CuO and Sn-9wt.%Zn-1wt.% $TiO_2$  denoted as S1,S2 and S3 lead free solder alloys were heat treated at 75, 100, 125 and 150°C with the accuracy of  $\pm 1^\circ C$  for two hours each, then slowly cooled inside a switched off furnace to obtain samples containing the fully precipitated phases and free from any plastic strain accumulation during machining.

The creep tests for the three different alloys were conducted using a computerized tensile testing machine under different applied stresses (5.0, 5.5, 6.0, 6.5 MPa) at room temperature. The structure of S3 alloy heat treated at the above temperatures has been examined using X-ray diffraction (XRD) using Philips X' Pert (MPD) goniometer PW3050/00 with graphite monochromatic using Cu-K $\alpha$  target and Ni filter operated at (40 K.V.) and (30 mA) to give a radiation of wave length ( $\lambda = 0.15406$  nm). The morphological characteristics of the three original alloy samples (S1, S2, S3) were examined by scanning electron microscope (SEM) and (OM). The appearances of the heat treated S3 alloy at the mentioned temperatures were studied by the optical microscope (OM). A solution of 2 % HCl, 3% HNO<sub>3</sub> and 95 % (Vol.) Ethyl alcohol was used for etching of the samples.

## Results And Discussions

### Creep Properties

Tensile creep curves of S1, S2 and S3 lead free solder alloys aged at four different temperatures (75, 100, 125, 150°C) and under various constant applied stresses  $\sigma$  (5.0, 5.5, 6.0, 6.5 MPa) are represented in Fig.1(a, b, c). All the creep measurements were conducted at room temperature.

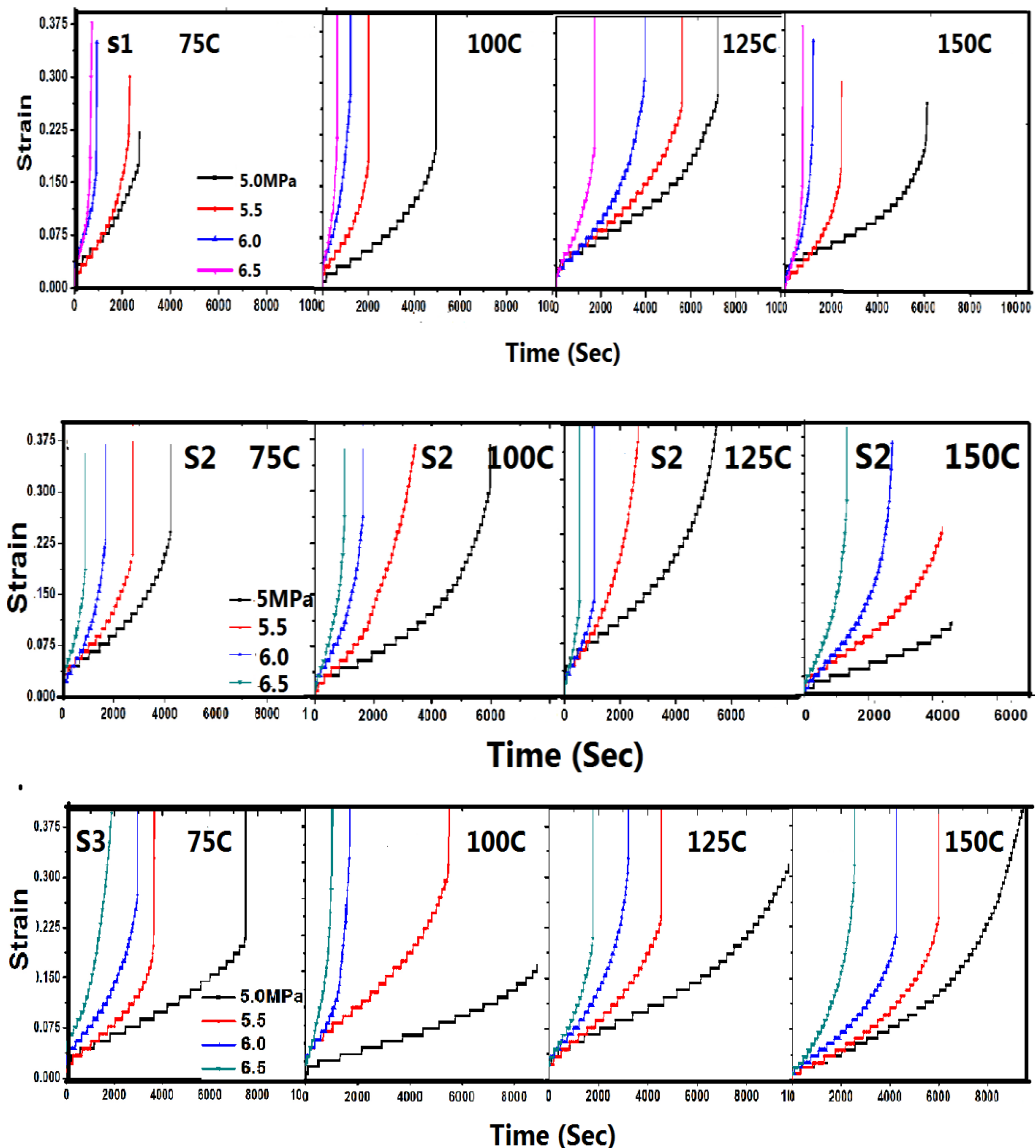


Fig. 1(a,b,c) : Creep behavior of S1,S2,S3 solder materials under different applied stresses (5.0, 5.5, 6.0, 6.5 MPa) and different aging temperatures (75, 100, 125, 150°C)

It is clear from the Figure that creep resistance is improved by the addition of CuO and / or TiO<sub>2</sub> and aging temperatures. The effect of TiO<sub>2</sub> shows a better creep resistance compared to that containing CuO. The creep curves and the corresponding

relationships between creep strain rates ( $\dot{\epsilon}$ ) and creep time of the three solder alloys aged at the (75&150°C) under constant applied stress of 6.0 MPa (as an example) are illustrated in Fig.2(a, b) respectively.

These curves display three different stages of creep behavior. Apparently, the shapes of the curves are

conventional, with a well-defined primary, secondary and tertiary creep deformation characteristic can be seen. The minimum creep rate  $\dot{\epsilon}$  variation suggests a basic change in the internal stresses. It is clear that the minimum creep rates decrease with particle additions (CuO, TiO<sub>2</sub>); which indicates that these particles reinforced the Sn-Zn alloy matrix. The creep resistance is further reinforced by the incorporation of TiO<sub>2</sub> particles (S3). The creep tests of S<sub>3</sub> alloy samples, treated at four different aging temperatures (75,100,125,150°C) and crept under 6.5 MPa (as an example) are shown in Fig. (3a).

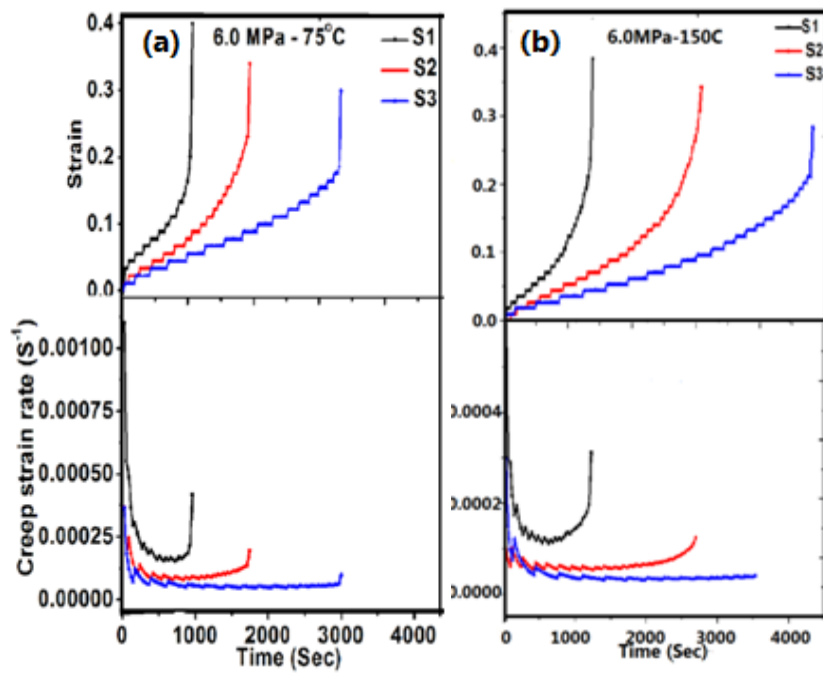


Fig. 2 (a, b) : Representative curves for the three solder alloys aged at (75, 150 °C) and their corresponding relationship between creep strain rate versus time (sec).

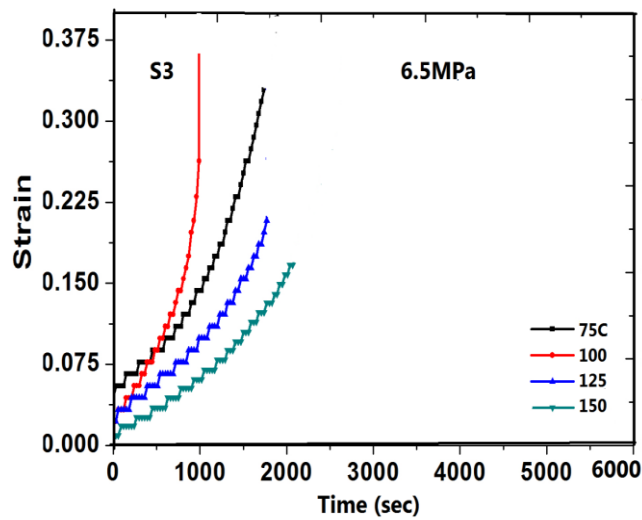


Fig. 3 (a): Strain-time relationship for S3 solder alloy treated at different aging temperatures and crept under 6.5MPa

The dependence of steady state creep rate  $\dot{\epsilon}_s$  on the applied stress ( $\sigma$ ) and temperature (T) is expressed as in previous studies [27] by:

$$\dot{\epsilon}_s = A \sigma^n \exp(-Q/RT) \quad (1)$$

Where, A is a complex constant depending on the material structural properties. Taking the natural logarithm on both sides of equation (1), we get:-

$$\ln \dot{\epsilon}_s = \ln A + n \ln \sigma - Q/RT \quad (2)$$

It is clear that at a given temperature, the creep stress exponent (n) can be calculated by linear regression of the experimental data. The stress exponent (n) values of the S3 solder alloy were found to be in the range (4.6–14.9), which is in agreement with those available in the literature [26, 28]. The reinforcement particles in the composite alloys served as effective barriers for dislocations movement and gave rise to the high stress exponent values obtained in this work. The relationship between the stress exponents (n) as a function of annealing temperature is shown in Fig. 3(b). From this Figure it is shown that the exponent value decreases with increasing temperature except at the aging temperature of (100 °C) which shows abrupt rises to 14.9.

#### Microstructure Analysis

X-ray diffraction patterns (XRD) were utilized to identify the effect of different aging temperatures (75, 100, 125, 150°C) on the deformed Sn-9.0

wt.%Zn-1.0wt.%TiO<sub>2</sub> (S3) lead free solder alloy at 6.0MPa shown in Fig. 4(a).

#### Microstructure Analysis

X-ray diffraction patterns (XRD) were utilized to identify the effect of different aging temperatures (75, 100, 125, 150°C) on the deformed Sn-9.0 wt.%Zn-1.0wt.%TiO<sub>2</sub> (S3) lead free solder alloy at 6.0MPa shown in Fig. 4(a).

The XRD patterns show large peaks intensity of  $\beta$ -Sn rich phase & small peaks of Zn &TiO<sub>2</sub> (with rutile structure) for (S3) alloy heated at 75°C as an example. The phases with card no. 01-089-2958, 01-089-0713 and 00-001-1292 for Sn, Zn and TiO<sub>2</sub> respectively are marked in Figure (Fig.4(b)).

The lattice parameters ( a, c, c/a,  $\Delta c/c_0$  ) are calculated and illustrated in fig.4(c, d, e). The peak height intensities of some crystallographic plains (200), (400) are illustrated in Fig. 4(f).

The apparent crystallite size L(nm), lattice strains  $\epsilon$  and dislocation density of the (101) plain that were calculated in previous works [29,30] are illustrated in Fig.4(g, h, i) respectively and their values are tabulated in Table (1). It is shown that all x-ray parameters follow the same trend of the creep behavior.

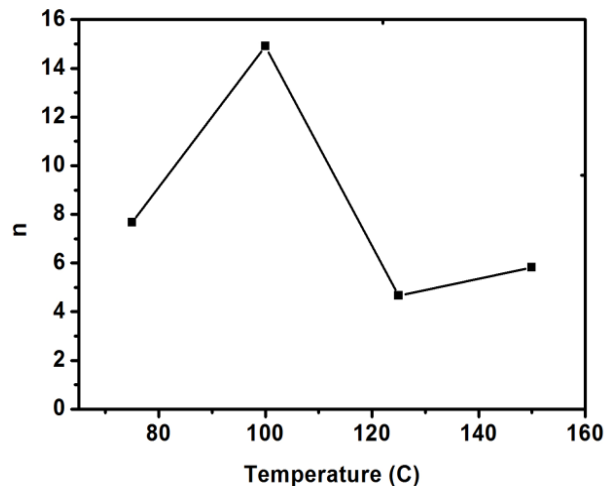


Fig. 3(b): Relationship between creep (n) exponent and aging temperature for Sn-9wt.%Zn-1wt.%TiO<sub>2</sub> 3solder alloy (S3)

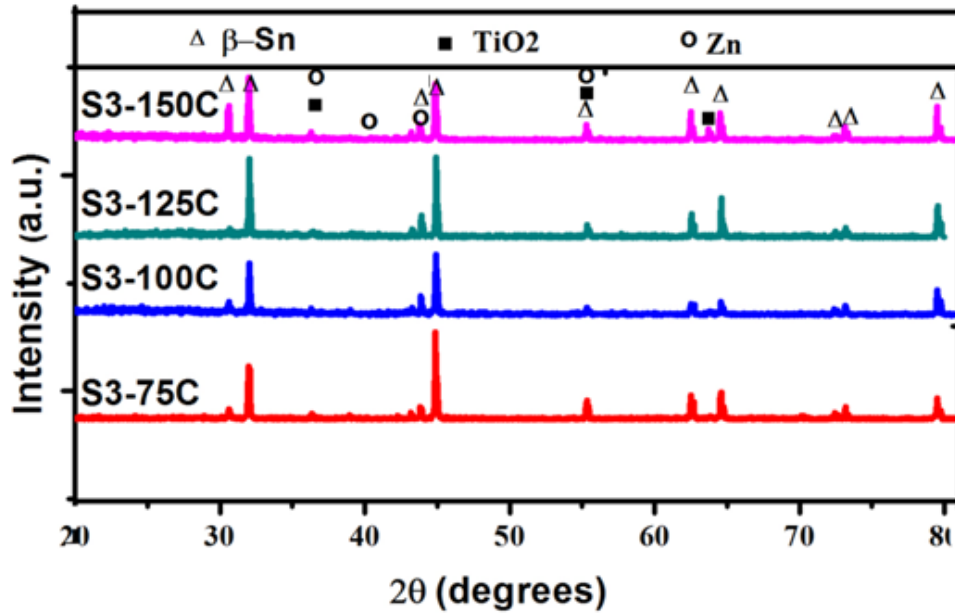


Fig. 4(a): x-ray diffraction patterns for S3 solder alloy crept at (5.0 MPa) and at different aging temperatures

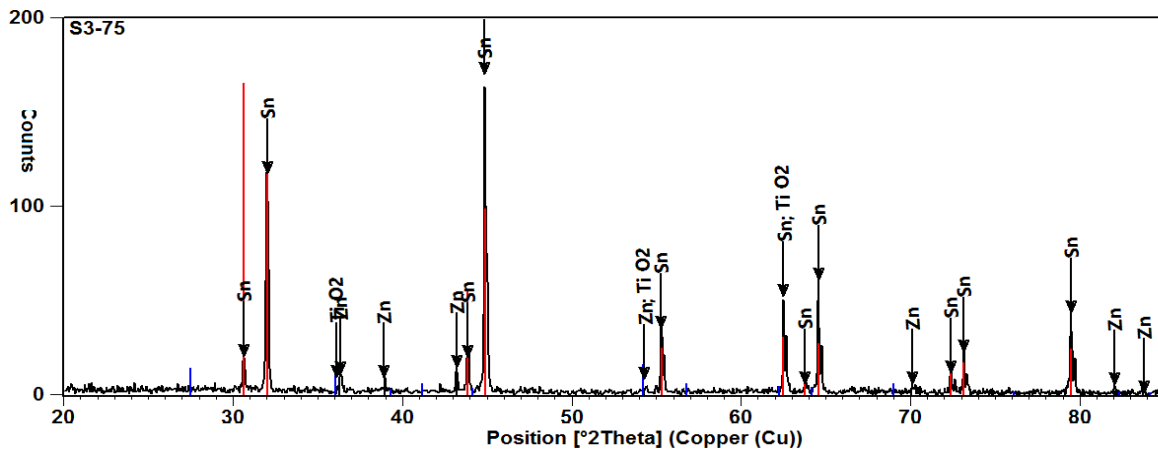


Fig. 4(b): Peak – position of Sn-9wt.%Zn-1wt.% $\text{TiO}_2$  solder alloy (S3) aged at 75°C

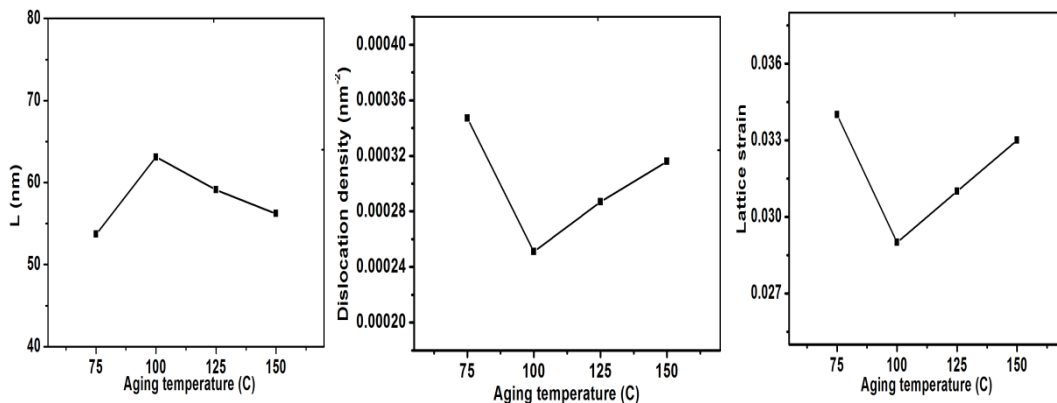


Fig. 4(g, h, i): The variations of the crystallite sizes, lattice strains and dislocation densities as function of the aging temperatures

### Morphological Studies

The microstructure of Sn-Zn solder alloy consists of a mixture of Sn-rich phase and Zn precipitated at the grain boundaries. The scanning electron microscope (SEM) micrographs of S1, S2 and S3 solder alloy before creep tests are shown in Fig 5(a).

From Fig.5a, the S1 sample exhibited dendrite dark regions and inter dendrite bright regions, the bright regions is expected to be  $\beta$  Sn phase. The S2

sample shows a needle-like structure which is expected to be CuO arranged in densely packed areas. These areas are interpreted by relatively large  $\beta$  Sn inclusions. Addition of TiO<sub>2</sub> shows flowers and an eye-like shape dispersed throughout the whole specimen (S3), which stabilize the grain microstructure, restrain grain growth effectively, act as pinning centers for dislocation movements and enhance the creep resistance of the solder material.

**Table (1): The crystallite size (L), lattice strain ( $\epsilon$ ) and dislocation density ( $\rho$ ) normal to (101) plane as a function of aging temperatures**

Temperature (°C)	L(nm)	( $\epsilon$ )	( $\rho \times 10^{-4}$ )
75	53.70	0.034	3.47
100	63.11	0.029	2.51
125	59.06	0.031	2.87
150	56.24	0.033	3.16

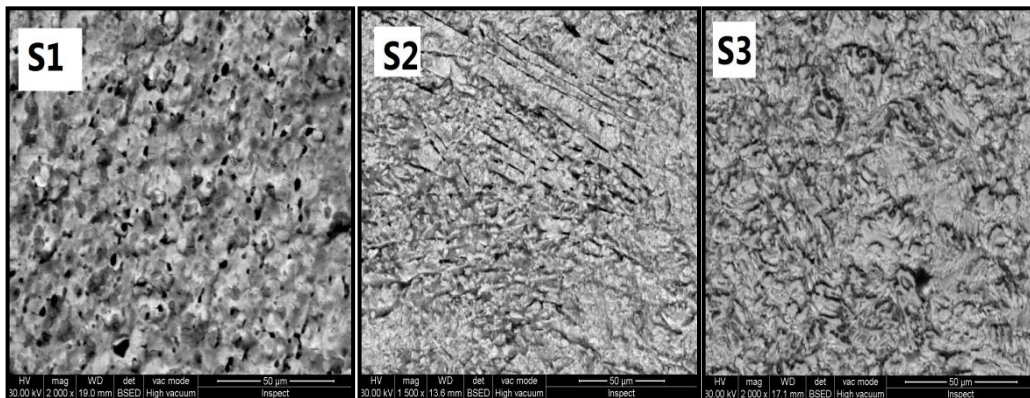


**Fig. 5(a): Scanning electron microscope of un-deformed S1, S2, S3 alloys**

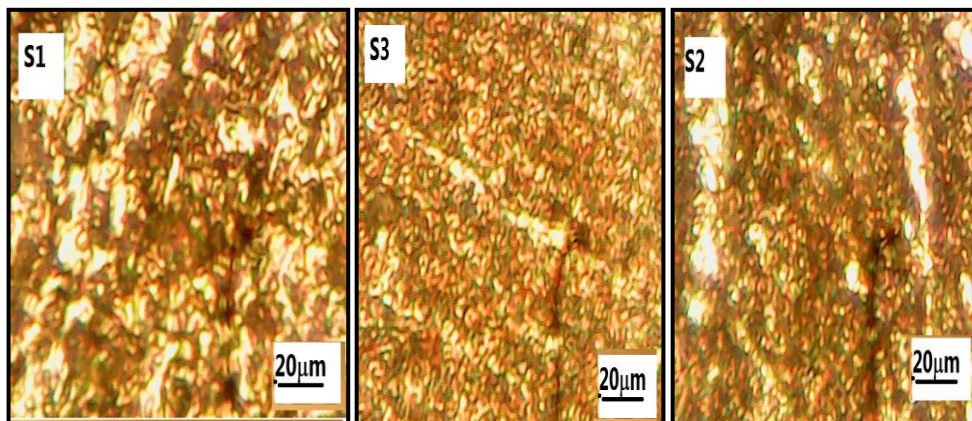


**Fig. 5(b): (OM) microstructures of un-deformed S1, S2, S3 solder alloys**

Fig. 6(a-d) depicts the microstructure of the S3 alloy samples thermally aged at the four different temperatures. The optical micrograph shows that the grain size increases with increasing aging temperature up to 100C then decreases at 125C, then it becomes nearly constant which in agreement with x- ray parameters. The grain

diameter as a function of temperature is measured by the intercept method reported by Braunovic and Haworth [31] and is shown given in Fig. 6(e), which follows the same behavior of all the studied parameters.

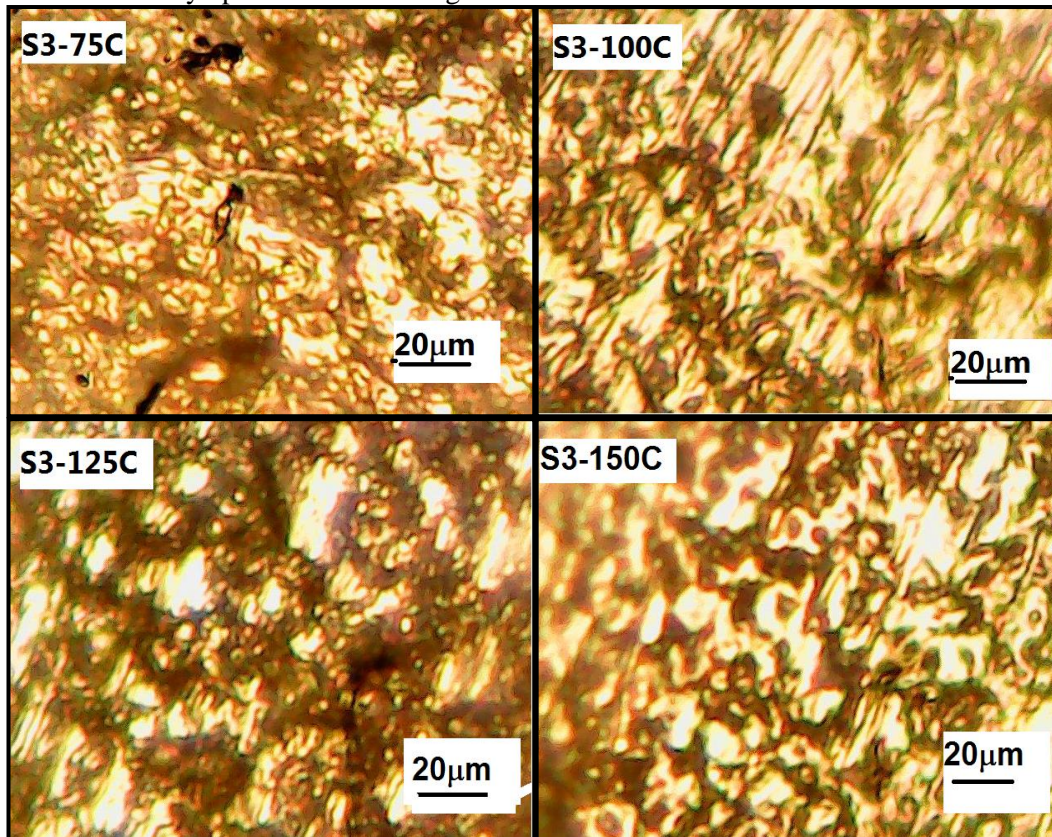


Fig. 6 (a-d): OM microstructures of un-deformed S3 solder alloy aged at different temperature (75, 100, 125, 150 C) respectively

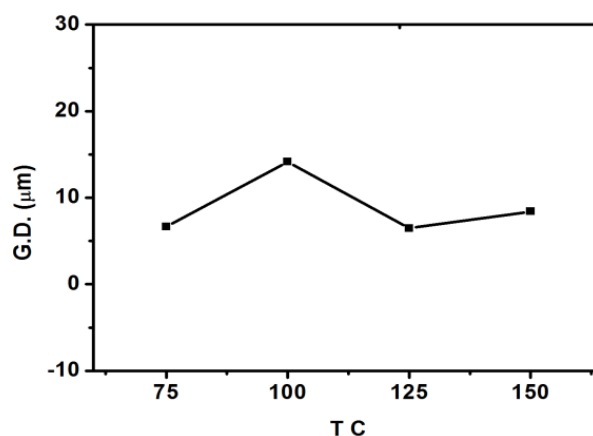


Fig. 6 (e) Dependence of grain size of the Sn-9wt.%Zn-1wt.%TiO<sub>2</sub> solder on the aging temperatures

## Conclusion

The effect of nano-sized reinforced additions on microstructure and creep properties of Sn-9wt. % Zn lead-free solder alloy was studied and the results show that the additions of CuO and /or TiO<sub>2</sub> nano particles to Sn-9wt. % Zn lead free eutectic solder alloy shows modification in the creep resistance and microstructure investigations. The Creep resistance of Sn-9wt. % Zn lead-free solder alloy is also improved by the type of addition. The microstructure reveals that the addition of CuO nano-particles leads to a needle-like structure characterized by large  $\beta$ -Sn inclusion, which pin the grain boundaries in the solder, stabilize the microstructure and strengthen the matrix. The addition of TiO<sub>2</sub> nano particles was found to be helpful in enhancing the overall strength of the eutectic solders. The mean value of the stress exponent of the Sn-9wt.%Zn-1wt.%TiO<sub>2</sub> solder shows a successive decrease with temperature except at 100C due to dissolution of Zn .

## References

- 1-YS. Lai, HM. Tong, KN. Tu.K. Recent research advances in Pb-free solders, *Microelectron Reliab*, 49, (2009) 221-2.
- 2-BHL Chao, X. Zhang, SH. Chae, PS. Ho Recent advances on kinetic analysis of electromigration enhanced intermetallic growth and damage formation in Pb-free solder joints. *Microelectron Reliab* 49, (2009) 353-63.
- 3-J.Shen, YC. Chan, Research advances in nanocomposite solders. *Microelectron Reliab* 49, (2009) 223-34.
- 4-YW. Wang, YW lin, CR.Kao, Kirkendall voids formation in the reaction between Ni-doped SnAg Pb-free solders and different Cu substrates. *Microelectron Reliab* 49, (2009) 248-52.
- 5-M.Date, T. Shoji, M. Fujiyoshi, K. Sato, KN. Tu Ductile-to-brittle transition in Sn-Zn solder joints measured by impact test *Scr Mater* , 51 (2004) 641-5.
- 6-J. Shen, Y.C.Chen, *Microelectron. Reliab.* 49 (2009) 223-234.
- 7-L.C. taso, S.y. Chang, *Mater.* 31 (2010) 990-993.
- 8-L.C.Taso, S.Y. Chang, C.I. Lee, W.H. Sun, C.H. Hung, *Mater.* 31 (2010) 4831-4835.
- 9-J. Shen, Y.C. Lue, D.J. Wang, H.X. Gao, *J. Mater. Sci. Technol.* 22 (2006) 529-532.
- 10-X.L. Zhong, M. Gupta, *J. Phys. D: Appl. Phys* 41 (2008) 095403-095409.
- 11-K. Mohan Kumar, V. Kripesh, A.A.O. Tay, *J. Alloys Compd.* 450 (2008) 229-237.
- 12-S.M.L. Nai, J. Wei, M. Gupta, *Mater. Sci. Eng.* A423 (2006) 166-169.
- 13-S. M. L. Nai, J. Wei, M. Gupta, *Thin Solid Films* 504 (2006) 401-404.
- 14-L.C. Taso, C.P. Chu, S.F. Peng, *Microelectron. Eng.* 88 (2011) 2964-2969.
- 15-M.Mc Cormack, S. Jin, *New Lead Free Solders. J. Electron Mater.* 23 (1994) 635-40
- 16-L.C. Taso, S.Y.Chang, *Mater* 31 (2010) 990-993.
- 17-L.C. Taso, S.Y. Chang, C.I. Lee, W.H. Sun C.H. Hung *Mater* 31 (2010) 4831-4835.
- 18-T. Shrestha, S. Gollapudi, I. Charit, and K.L. Murty, *J. Mater. Sci.* 49, (2014) 2127.
- 19-[19] H. Mavoori, T. Chin, S. Vaynman, B. Moran, L. Keer, and M Fine, *J. Electron. Mater.* 26, (1997) 783.
- 20-[20] N. Hamada, M. Hamada, T. Uesugi, Y. Takigawa, and K.Higashi, *Mater. Trans.* 51, (2010) 1747.
- 21-[21] A.A. El-Daly, A.E. Hammad, G.A. Al-Ganainy, and A.A.Ibrahiem, *Mater. Des.* 56, (2014) 594.
- 22-[22] G. Saad, A. Fawzy, and E. Shawky, *J. Alloys Compd.* 479, (2009) 844.
- 23-[23] S.K. As, A. Sharif, Y.C. Chan, N.B. Wong, and W.K.C.Yung, *Microelectron. Eng.* 86, (2009) 2086.
- 24-[24] F. Tai, F. Guo, J. Liu, Z. Xia, Y. Shi, Y. Lei, and X. Li, *Solder. Surf. Mount Technol.* 22, (2010) 50.
- 25-[25] W.Q. Xing, X.Y. Yu, H. Li, L. Ma, W. Zuo, P. Dong, W.X.Wang, and M. Ding, *Mater. Sci. Eng., A* 678, (2016) 252.
- 26-[26] A.M.Yassin, H.Y.Zahran and A.F.Abd El-Rehim, Effect of TiO<sub>2</sub> Nanoparticles Addition on the Thermal, Microstructural and Room-Temperature Creep Behavior of Sn-Zn Based Solder, *Journal of Elec Materi* 47 (2018) 6984-6994.
- 27-[27] B.A.Khalifa, R. Afify Ismail, A.Yassin, " Structure Analysis, Enhancement of Creep Resistance and Thermal Properties of Eutectic Sn-Ag Lead-Free Solder Alloy by Ti and Cd Additions" , *Journal of Advances in Physics*, Vol. 8 ISSN: 2347, 3487 (2017) 5092-5099.
- 28-[28] R. Mahmudi, AR. Geranmayeh, H.Noori, M. Shahabi. Impression creep of hypoeutectic Sn-Zn lead-free solder alloys. *Mater Sci. Eng. A;* 491, (2008) 110-116.
- 29-[29] R. Afify Ismail, A.M. Yassin, B.A. Khalifa, "Investigation of Microstructure and Creep Properties of Sn-xSb Solder Alloys up to Peritectic Composition", *Journal of Advances in Physics* Volume 15 ISSN: 2347, 3487 (2018) 5970-5982.
- 30-[30] B.A. Khalifa, R. Afify Ismail, A.M. Yassin, "Indentation Creep and Microstructure Properties of Sn-Ag Solder Alloys", *Journal of Advances in Physics*, *Journal of Advances in Physics* Vol 16 ISSN: 2347-3487 (2019) 171-184.
- 31-[31] M. Braunovic and C.W. Haworth, *J. Appl. Phys.* 40, (1969) 3459